Systems Approach for Evaluating Dynamics and Plantwide Control of Complex Plants

Alexander J. Groenendijk, Alexandre C. Dimian, and Piet D. Iedema
Universiteit van Amsterdam, Instituut voor Technische Scheikunde, 1018 WV Amsterdam, The Netherlands

Recycle loops strongly affect dynamics and control of complex plants. The stability of control structures for component inventories may be influenced by recycle interactions and by connectivity, which leads to flowsheet alternatives possessing different control properties. A simulation-based methodology for evaluating these phenomena and finding the best flowsheet structure is reported from a controllability point of view. Steady-state and dynamic simulations are combined with controllability analysis tools, both steady state and in the frequency domain, which extracts more value from simulation than the usual sensitivity studies. The case of a vinyl chloride monomer (VCM) plant with impurities handling as a main issue demonstrates the power of the approach. It leads to an unconventional design alternative where an extra impurity-destroying reactor reduces bad dynamic characteristics, since it prevents impurity buildup in the recycle. The steady-state analysis of the VCM case is confirmed at low frequencies of disturbances, but difficulties may occur at higher frequencies, where the disturbances' period and time constants of the distillation columns are of the same order of magnitude. Controller interactions play a significant role in disturbance rejection. Nonlinear dynamic simulations with closed plantwide control loops confirm the analysis results.

Introduction

Nowadays, design practices that address complex integrated plants are well established as far as the steady state is concerned. However, analysis of plant dynamics during the conceptual design stage leading to better flowsheet alternatives from the controllability point of view is a recognized, but unresolved problem. Also in process systems science attempts to incorporate dynamics in the development of methods for process flowsheet synthesis are barely available (Mohideen et al., 1996). Clearly, a systematic analysis of plantwide dynamics and controllability is difficult, partly because of the effect of recycles. As Luyben noted ''Processes with recycle streams are quite common but their dynamics poorly understood'' (Luyben, 1993a). This is crucial in the context of *zero-discharge plants*, where even more material has to be recycled. A complex plant may involve strong interactions between recycle loops that sometimes lead to a significant influence on the performance of individual units. Therefore, a real need exists to find a quantitative methodology to analyze the effects of interactions. Flowsheeting is a well-established technique reflecting the complexity of systems by means of an accurate, steady-state plant model (Dimian, 1994). The current practice in the analysis of large plants seems to be limited to the exploration of the *operating window* by such flowsheeting. However, more essential design and operation knowledge is obtained through dynamic flowsheeting, since it accounts for control features. In addition, large dynamic plant models in principle give access to a whole class of controllability tools that usually are applied to small problems. However, this requires an adequate reduction of these models, which is not a trivial problem as will be discussed in a forthcoming publication. The goal of this article is to present a methodology to combine large dynamic models with controllability tools and to demonstrate their use by means of a practical problem: the dynamics of the plant material balance, and particularly that of impurities.

The objective of our approach is to obtain a quantitative measure of the plant performance using reference tracking and disturbance rejection in an early design stage. A better

Correspondence concerning this article should be addressed to A. C. Dimian.

understanding of dynamic interactions between recycles is desired, from which design modifications with improved operability characteristics are more readily invented without using complex control strategies. We therefore use simple proportional feedback-control and controllability tools in addition to extensive steady-state and dynamic simulations. A complex multivariable control system may be implemented afterward, but this is beyond the scope of this article. Controllers and controllability tools are only used to measure the performance of the design and to find the effect of design modifications.

In a case study about the handling of impurities in a complex plant, it is demonstrated how connectivity between units and interactions between recycles can be exploited to create flowsheet alternatives with plantwide control structures that would be infeasible in a stand-alone unit (Dimian et al., 1996). The control structures may imply variables belonging to different units. The controllability properties are determined by the competition between *positive feedback* effects, typically recycles, and *negative feedback* effects, like exit streams and chemical reactors. In this example an extra reactor is introduced, where impurities that are difficult to handle are transformed into other components. Since these components are easily removed from the recycle, the closed-loop performance of the system is improved with respect to disturbance rejection. In future work we will investigate alternative recycle structures and their controllability properties.

Interaction Between Design and Control

Gilliland et al. (1964) started the study of the reactor/separator system, which is the basic couple in a flowsheet. They showed that the overall dynamics may strongly differ from the dynamic behavior of individual units. In general, it was found that a recycle increases the process response time and sensitivity to disturbances (positive feedback). Later Verykios and Luyben (1978) considered the same problem with separation dynamics, demonstrating that the recycle may also exhibit underdamped behavior. Denn and Lavie (1982) found that resonant peaks can occur in the frequency response when the recycle path contains a time delay, while these were of the same order of magnitude as the plant steady-state gain. Papadurakis et al. (1987) also studied the simple reactor/separator system and found that RGA for isolated units is insufficiently reliable to give a correct measure of interactions in the flowsheet.

Buckley (1974) invented the first synthesis methodology for plantwide control systems based on the dynamics of the material balance, which proved to be fruitful in the industry. Price has reported an improvement in this methodology with respect to throughput control (Price et al., 1994). Downs (1992) has demonstrated the importance of component inventory for plantwide control strategies. In this respect the importance of purge placement (Joshi and Douglas, 1992) also should be mentioned.

Luyben (1993a,b,c) and Luyben and Tyreus (1993) started a more systematic study on the rationale of recycle systems dynamics, demonstrating that recycle and reactant feed or makeup policies are interrelated. He proposed an important generic rule for designing plants with recycle streams: ''fix some flowrate somewhere in the material balance recycle loop.'' Consequently, new reactor feed procedures with superior operability properties may be considered. Luyben studied the application of these guidelines to more complex flow sheets (Luyben and Luyben, 1995), finding that the reaction steps and inventory regulation of intermediate species affect the operability. Some control structures can have multiple steady states and produce closed-loop instability.

The use of open-loop controllability measures an evaluation tools in conceptual design has been promoted by several authors (Barton et al., 1991; Mizsey and Fonyo, 1991; Lyman and Georgakis, 1995; Morud and Skogestad, 1993; Wolff and Skogestad, 1992). Morud (1995) studied the dynamics of some basic elements of a complex plant, while Wolff (1994) emphasized controllability measures applied to recycle systems. Skogestad and Poslethwaite (1996) gave an overview of multivariable feedback control.

Although considerable progress has been reported in the literature mentioned, it is not obvious how to obtain profit from these tools in the design of real complex plants. Both analytical investigations using simplified models, as well as industrial case studies with design and thermodynamic constraints, should contribute to a systematic methodology for integration of conceptual design and plantwide control. Most work has been performed only on *how to evaluate* existing design alternatives, but little on *how to design* the plant in order to meet controllability and flexibility requirements. This remains a big challenge.

Systems Approach

A systematic approach (Table 1) has been developed for the combination of steady-state and dynamic simulations with controllability analysis tools that is applicable to both new design and revamping existing structure. Design freedom is used to improve the controllability properties of the plant.

The approach starts with a definition of the objectives of the plant and identification of the inputs, outputs, targets, and constraints. Then a rigorous steady-state simulation model is developed. This is calibrated at a nominal operating point, where the system satisfies all targets and constraints. The input/output behavior is studied around this point through exploration of the operating window. At this stage a selection of the variables to be controlled during the operation and those to be manipulated in a control structure is made. These variables are normally related to the design specifications and the design variables. Steady-state RGA and SVD analyses are used to evaluate the plantwide control structure alternatives.

The next step is the development of a rigorous dynamic model incorporating the main design and control features, as detected by the steady-state analyses. Rigorous dynamic models require information of equipment sizes and basic level as well as pressure control. Since dynamic models usually are too large and complex for controllability analysis, these have to be simplified and linearized.

The dynamic model is linearized either by identification of generated input/output responses, giving a set of transfer functions, or by a state-space realization. The inputs and outputs are scaled between their allowed minimum and maximum values (outputs, manipulated variables) or expected

Table 1. Systems Approach

Problem definition
- Operating window; inputs, outputs, targets, constraints

Calibration of steady-state plant-simulation model
- Rigorous modeling
- Detailed material balance around operating point

Plantwide control objectives
- Control variables
- Manipulated variables
- Disturbances
- Scaling

Steady-state analysis
- Static-gain calculations
- RGA and SVD
- Evaluation of control structure alternatives

Dynamic flowsheeting
- Development of a reduced model, which incorporates the main design and dynamic features of the complex plant detected by steady-state analysis
- Dynamic responses of system on perturbations

Dynamic analysis
- Linear dynamic model as a set of transfer functions (identification method) or a state-space description (model-based)
- Frequency analysis
  Bode diagrams for stability and crossover frequencies
  RGA and RGA number for control structure design
  PRGA, CLDG, and RDG for controllability performance
- Evaluation of control structure alternatives
- Proportional controller gains

Closed-loop simulation
- Implementation and (fine)tuning of proportional controllers
- Dynamic simulation
- Evaluation of control-structure alternatives

Design alternatives
- Unit operations
- Recycle structure alternatives

Conclusions
- Recommendation of flowsheet design
- Suggestions for plantwide control strategy

(disturbances) (Skogestad and Postlethwaite, 1996). Thus, all variables obtain values in the interval $[-1, 1]$. Bode plots of the linear models show the frequency at which the dynamic behavior of the plant starts to differ from steady state as well as the crossover frequencies up to which feedback control should be active. In order to study the closed-loop behavior, a certain control structure has to be assumed. In this approach a decentralized control structure is selected that contains only control loops with one input and one output. Furthermore, the inputs and outputs are arranged in such a way that the proportional gains in the corresponding controller matrix are on the diagonal, which explains the synonym ''diagonal'' control.

The RGA number is used to see whether the preferred diagonal-control structure detected from the steady-state analyses works well over the whole frequency range of interest. The performance relative gain array (PRGA), closed-loop disturbance gain (CLDG), and relative disturbance gain (RDG) are used as indicators for the performance of the diagonal control structure according to reference (setpoint) tracking and disturbance rejection. Interactions between the controllers in a diagonal structure are also taken into account by these indicators (Skogestad and Postlethwaite, 1996).

The controllability analysis is supposed to produce an optimal control structure. This structure is implemented in the full nonlinear dynamic model. Controllers are being fine-tuned first, and then a closed-loop simulation is performed. Analyzing and understanding the dynamic behavior of a model generates suggestions for improvement. The procedure described may be applied on several flowsheet alternatives, finally yielding an optimal flowsheet design and suggestions for a plantwide control strategy.

Case Study

Problem definition

The removal of impurities in a balanced VCM process is known to be difficult. Significant market fluctuations require a wide operating window, while maintaining product purity under economical conditions. Higher reaction conversion or plant throughput typically yields more secondary products and impurities that may accumulate and cause unstable operation.

The main reactions in the process are as follows:

Chlorination

$$C_2H_4 + Cl_2 \rightarrow 1,2\text{-}C_2H_4Cl_2(\text{DCE}) + \text{impurities}$$

Cracking

$$\text{DCE} \rightarrow C_2H_3Cl\ (\text{VCM}) + HCl + \text{impurities}$$

Oxychlorination

$$C_2H_4 + 2\,HCl + 1/2\,O_2 \rightarrow \text{DCE} + H_2O + \text{impurities}$$

Waste and impurities in the effluent of the three reactors may originate from (1) feed impurities, (2) secondary reactions with the main reactant(s), and (3) supplementary reactions with feed impurities. Each reaction section may have its own separation system, but some of the impurities from different reactors may be collected and eliminated in a central separation system. Recycling of impurities over more than one reactor may generate even more waste material. In general, impurities lead to operation problems. Their upper concentration limit must be strictly controlled to prevent polymerization or fouling. In special cases, however, some impurities may be useful catalyzing or inhibiting desired reactions, and their concentrations have to be kept at an optimum value by balancing formation and elimination rates. Thus, impurity control and main-component control are strongly coupled. A special feature of impurity dynamics is the fact that some of them are always in transient state, hence a simultaneous steady-state optimization of both is impossible. However, an accurate steady-state plant simulation model does help to quantitatively understand and evaluate formation and elimination mechanisms as well as interactions between these.

Figure 1 presents the flowsheet. The reactions take place in reactors R1 (chlorination), R2 (cracking), and R3 (oxychlorination). The washing/drying section S0 removes unconverted reactants. A first amount of (light) impurities is removed by column S1. Three main recycle loops cross in the

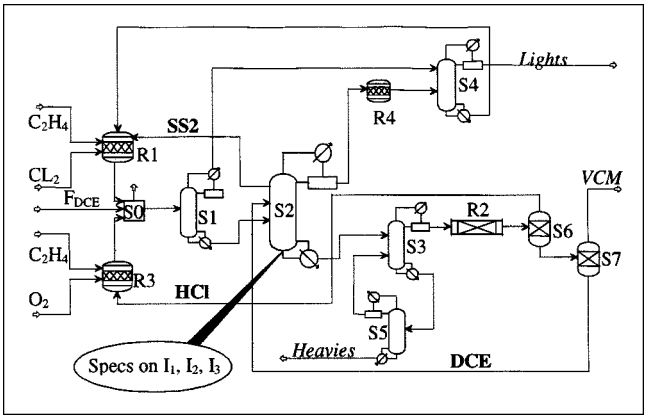

Figure 1. Balanced VCM process with optional reactor R4.

distillation column S2 whose main function is to purify fresh and recycled DCE. Three other distillation columns are involved in this operation: S3 for finishing DCE, S4 for ''lights,'' and S5 for ''heavies'' removal. Column S2 also collects impurities associated with the production and the recycling of DCE, which may contain lights, intermediates, and heavies. Among the impurities three significant components are identified for this process: chloroprene (I_1), trichloroethylene (I_2), and CCl_4 (I_3). These components are lighter than the main component DCE. Both I_1 and I_2 are polymerizable and are subject to concentration constraints in the bottom product of column S2. They may leave the plant as lights via column S4, but significant amounts will remain in the recycle to reactor R1. There they are transformed into heavies (C_4Cl_6) that are easily removed by column S5. They are also drawn as a side stream from column S2, being directly recycled to the reactor R1. This creates a fourth loop, also containing S2. They may also be destroyed in a supplementary reactor R4, between columns S2 and S4. This will decrease the impurity loading of S4, which will improve its performance. Therefore, this alternative design may have better control properties.

A major feature of the VCM process is the fact that impurity I_3 has a beneficial role since it enhances both conversion and yield of the cracking reaction. I_3 will leave the system only via column S4 as lights. Therefore, regarding the removal of I_1 and I_2, a compromise has to be found, with an optimal concentration of I_3 in the bottom of the column S2. These considerations show that the design and operation of S2 are essential for the process as a whole. S2 is a large distillation column, operating at a very large reflux ratio (Table 2). Its operation is constrained by specifications on the quality of the bottom product: $spec_1$ the maximum concentration of I_1, $spec_2$, the maximum concentration of I_2, and $spec_3$ the optimum concentration of I_3.

Plantwide control strategy

In a complex plant like the balanced VCM process, a large number of variables have to be controlled. Most of them—pressures, temperatures, levels—may be controlled locally. However, material balances in general and especially the material balances of impurities are established by interactions between the different operating units and recycles in the plant. Therefore, the control of all material balances requires a plantwide approach.

Consequently, the handling of impurities is dealt with as a multivariable control problem. Here the controlled variables (*outputs*) are maximum or optimum values of concentrations (flow rates) of impurities on selected streams or locations. They may be measured in an operating plant, but also be set as ''design specifications.'' These specifications can be achieved by manipulating *inputs* as distillate flow rate, reflux ratio, reboiler duty, feed temperature, and so on. These may also be interpreted as ''design variables'' in a new design or revamp. It is obvious that one manipulated variable affects more than one controlled variable, so interaction between controller loops should be taken into account.

In this study we focus our attention on the material balances of the impurities I_1, I_2, and I_3. Since these have a slow dynamic behavior, the fast control loops are assumed to operate instantaneously. Therefore pressures, temperatures, and

Table 2. VCM-Plant Model Characteristics

Reactor	R1	R2	R3	R4	
Temperature (°C)	80	650	270	80	
Pressure (bar)	3	3	1	3	
Dynamic	Rigorous	Instantaneous	Instantaneous	Rigorous	
Column	**S1**	**S2**	**S3**	**S4**	**S5**
No. of stages	6	47	6	10	13
Feed stage(s)	2	22/37	3/5	3/5	6
Distillate (kmol/h)	4.5	14.5	1,896.5	5.59	60
Reflux (kmol/h)	6.75	957	1,327.5	33.67	70
Side draw (kmol/h)		35 (stage 5)			
Bottom (kmol/h)	1040	1900	65	13.25	5.23
Q_{reb} (GJ/h)	1.4	34	100	1	3.7
Pressure top (bar)	1.4	1.4	3	1.11	0.20
2nd stage	1.415	1.415			
Bottom	1.5	2.315	3.1	1.36	0.25
Temp. top (°C)	94.2	83.4	123.1	65.3	39
Bottom	96.7	112.8	127.6	91.45	125.6
Dynamic	Rigorous	Rigorous	Rigorous	Rigorous	Rigorous

Note: Thermodynamic model: UNIQUAC; number of components: 13 (only 6 in separation system of dynamic model). Steady-state model in ASPEN Plus 9.3; dynamic model in SPEEDUP 5.5.

levels are fixed in the simulation models, while duties and flow rates are free (calculated). In the distillation columns we assume that the reflux flow is used to control the drum level and the bottom flow to control the reboiler level. The reboiler duties and distillate flow rates are used to meet the specifications.

A steady-state plant model is used to find the nominal operating point. By trying to satisfy the specifications on the impurities I_1, I_2, and I_3 in the bottom product of column S2 (*outputs*), the important role of column S4 as an exit of impurity I_3 became evident. Simulations did not converge with a too small distillate flow rate. Impurity I_3 is then built up in the plant ("snowball effect" on impurities concentration; see also Figure 4). D4 is the only location where light impurities can leave the system. Therefore, D4 should be used to control the level of these lights. So, in addition to the column S2 distillate flow rate (D2), side-stream flow rate (SS2), and reboiler duty (Q2), the column S4 distillate flow rate (D4) and reboiler duty (Q4) are also taken into account as possible manipulated variables in a plantwide control structure (*inputs*). The main disturbance of the plant is the throughput, being modified by the flow rate of the external DCE feed (F_{DCE}). A second disturbance taken into account is the fraction of impurity I_3 in this stream (X_{I_3}).

Steady-state analysis

Basic Flowsheet. From extensive steady-state simulations a scaled gain matrix G is generated according to the relation $c = Gm$, where c are the scaled plantwide control variables and m are the scaled manipulated variables (Table 3). With the scaled disturbances d, a scaled disturbance gain matrix G_d is generated, according to the relation $c = G_d d$. The introduction of scaled variables allows reformulation of the plantwide control problem. Control is necessary to keep the impurities within their bounds under disturbances, since the scaled disturbance gains are greater than one.

When regarding the sign of the input/output gains, it is noticed that both D2 and SS2 have a negative effect on impurities I_1 and I_2, while the effect on I_3 is positive. Increasing these manipulated variables means recycling more material through reactor R1. Impurities I_1 and I_2 are transformed into heavies here ("negative feedback"), but I_3 is built up in the recycle ("positive feedback"). Increasing the reboiler duty Q2 will give rise to fewer impurities in the bottom product. This also holds for the distillate flow rate and reboiler duty of column S4 (D4, respectively, Q4). The first is an exit for the impurities, while the second will purify the recycle stream to R1, so both have a reverse effect on the controlled variables. The high-gain values are in line with their important role in removing impurities, especially for I_3.

Table 4 resumes the steady-state controllability analysis with RGA and SVD for five possible combinations of manipulated variables that have acceptable properties. The other combinations are not interesting, since they show large and negative RGA elements and high condition numbers. The large condition numbers indicate that the plant may be manipulated into certain directions more easily than into others. The lower singular values that are less than unity demonstrate that the outputs cannot be set independently. The RGA elements near unity suggest that diagonal control would be possible without too many interactions. The use of distillate flow rate (D4) or reboiler duty (Q4) from column S4 as manipulated variable to control impurity I_3 seems to give the best alternative control structures from a steady-state point of view.

Table 4. Static-Gain Indices of VCM Plant

I_1, I_2, I_3	RGA diag.	SVD	Cond. No.
Q2, SS2, D2	1.47, 1.56, 1.05	6.84, 0.50, 0.24	28.75
Q2, SS2, D4	1.47, 1.43, 1.01	6.91, 2.71, 0.31	22.04
Q2, SS2, Q4	1.47, 1.44, 1.01	6.84, 0.61, 0.31	22.30
Q2, D2, D4	1.43, 1.08, 0.86	6.90, 2.74, 0.16	41.83
Q2, D2, Q4	1.47, 1.18, 0.94	6.83, 0.74, 0.12	55.18

Flowsheet with Impurity-Destroying Reactor R4. Introduction of an extra reactor, R4, between columns S2 and S4 for the transformation of impurities I_1 and I_2 into heavies leads to a different steady-state system behavior. The heavies that are produced by reactor R4 will leave column S4 through the bottom, while impurities I_1 and I_2 left the system before as lights. Therefore, in this alternative design the concentration of impurity I_3 in the top distillate of column S4 is higher. To keep $spec_3$, the distillate flow rate of column S4 has been reduced about 40%. The nominal values of I_1 and I_2 become significantly lower, so their scaling factors are larger. The static gains for impurities I_1 and I_2 are therefore slightly reduced. The impact of the distillate flow rate on impurity I_3 is almost doubled (Table 5). Also the sensitivity of I_3 to the side-stream flow rate is increased by a factor of 5. This is the result of recycle interactions. I_3 is built up in all four recycle streams originating from column S2, and the only exit is the distillate flow of column S4. By reducing this exit, the sensitivity of I_3 to the recycle interactions is increased. This increasing sensitivity to recycle interactions is a remarkable result, especially relevant in the context of waste minimization and zero discharge plants, where impurities removal is even further reduced. It demonstrates that such design modifications meant to reduce waste have a strong impact on the performance of the system and may become detrimental in operation.

Table 6 shows the steady-state controllability indices for the alternative flowsheet. The higher RGA diagonal elements indicate slightly more interaction and the lower singu-

Table 3. Static-Gain Matrices of VCM Plant

	D2	SS2	Q2	D4	Q4	F_{DCE}	X_{I_3}
I_1	−0.075	−0.261	−5.742	−0.376	−0.079	4.424	0.132
I_2	−0.212	−0.527	−3.574	−0.437	−0.071	3.193	0.192
I_3	0.411	0.030	−0.893	−2.829	−0.616	2.606	1.631

Table 5. Static-Gain Matrices of VCM Plant with Reactor R4

	D2	SS2	Q2	D4	Q4	F_{DCE}	X_{I_3}
I_1	−0.076	−0.184	−4.325	−0.154	−0.041	3.303	0.096
I_2	−0.140	−0.302	−2.298	−0.215	−0.061	2.061	0.157
I_3	0.737	0.156	−0.908	−2.136	−0.727	2.237	1.853

Table 6. Static-Gain Indices of VCM Plant with Reactor R4

I_1, I_2, I_3	RGA diag.	SVD	Cond. No.
Q2, SS2, D2	1.49, 1.69, 1.12	4.99, 0.79, 0.15	33.67
Q2, SS2, D4	1.49, 1.39, 0.96	5.03, 2.05, 0.19	26.36
Q2, SS2, Q4	1.48, 1.40, 0.96	4.99, 0.73, 0.18	27.32
Q2, D2, D4	1.48, 0.95, 0.68	5.03, 2.17, 0.12	41.08
Q2, D2, Q4	1.45, 0.99, 0.71	4.99, 1.03, 0.09	58.43

lar values indicate a smaller operating window, but the differences are minor. We can conclude that on the basis of the steady-state analysis of both alternatives, no clear preference can be assigned to the different design and control alternatives.

Dynamic simulation

Identification of Main Dynamics. Prior to constructing a dynamic flowsheet, model decisions have to be made regarding the flowsheet elements whose dynamics have to be taken into account (Table 2 and Table 7). The steady-state analysis showed the important role of impurities destruction in reactors R1 and R4. Therefore, the impact of these two reactors on the plant dynamics is considered in this part, first for the basic flowsheet, and then for the flowsheet with impurity-destroying reactor R4. Reactors R2 and R3 are assumed to make no contribution to the plant dynamics, because being gas-phase reactors, they possess a negligible holdup and residence times with orders of magnitude of seconds or minutes only, and hence they are thought to act instantaneously.

The separation system is simulated dynamically with a reduced set of components. The reactants that have zero flow in the reactor outlet streams are omitted. Since phenomena concerning the impurity material balances take place at long time scales, level and pressure controllers are assumed to operate instantaneously. Therefore, condenser pressures are fixed and total material balances in drums and reboilers are modeled assuming steady state. So, condenser duties, reflux, and bottom flows are free, while reboiler duties and distillate flow rates are specified.

Basic Flowsheet. Dynamic simulations with step perturbations on the disturbances and manipulated variables show interesting responses (for the concentration of I_3 in the bottom of S2, see Figure 2). All impurities will finally reach steady-state values, but at different times. For steps for the distillate and side-stream flow rates of column S2, the manipulated variables D2 and SS2, respectively, new steady states are reached in about 24 h. The responses are influenced by the recycle interactions. In both cases recycle through reactor R1 is increased. More impurities I_1 and I_2 are destroyed, while, on the other hand, I_3 is being built up. After 2 h the concentration of I_3 will reach a maximum and then decrease to the final value. This is because impurity I_3 finally leaves the plant via column S4. Increasing the reboiler duty Q2 will boil out the impurities immediately. Recycles are responsible for a small increase after half an hour, but the steady state is reached within 2 h, which is faster than the responses on D2 and SS2.

Table 7. Dynamic Model Characteristics

	Base Case	With Reactor R4
System size	5780	5986
No. of equations/variables	4403	4534
No. of states	674	680

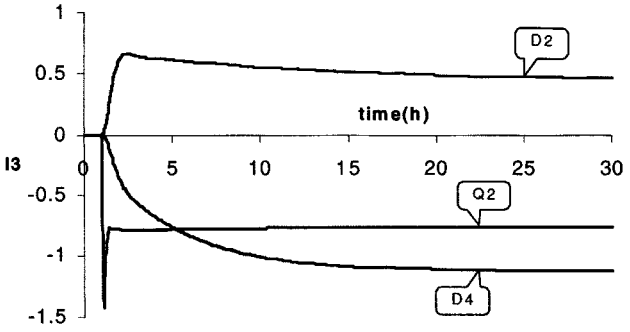

Figure 2. Dynamic response of impurity I_3 in the bottom of S2 after a scaled step perturbation of 1 on, respectively, D2, Q2, or D4 in the VCM plant.

Increasing Q2 gives an almost instantaneous drop of I_3, followed by a fast increase. The final value is reached much faster than after a step on D2 or D4. This is due to the time needed for recycles to reach equilibrium.

Simulations of an increase in distillate flow rate (D4) or reboiler duty (Q4) of column S4 show a decrease in impurities with a dualistic character, since the response is initially fast, but continues more slowly later on. The slowest part of the response is the more significant one, but it takes about 30 h to reach steady state. This is the time needed for all recycles to reach equilibrium. A similar dualistic response is observed from steps on disturbance variables (Figure 3): a long settling time of impurity I_3 after the same impurity increases in the external DCE feed (X_{I_3}) or in DCE feed flow (F_{DCE}).

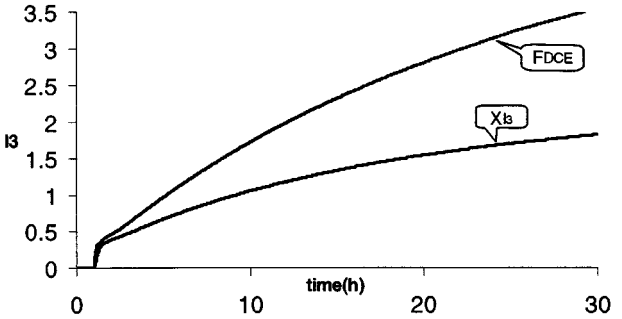

Figure 3. Dualistic response of impurity I_3 (bottom S2) after a scaled step perturbation of 1 on the external DCE feed F_{DCE} or impurity concentration I_3 in this feed, X_{I_3}, in the VCM plant.

When the DCE flow is increased, more VCM will be produced and more HCl, which is recycled and leads to a higher DCE production rate. The higher DCE rate gives rise to more production of impurities in the short term and to more buildup in the recycles in the longer term. An increase of the impurity content I_3 in the external DCE flow also yields more buildup in the recycles. The long settling time is due to the time needed for the recycles to reach equilibrium.

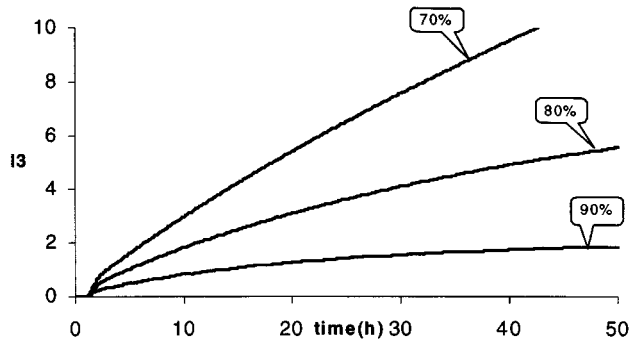

Figure 4. Snowball effect of D4 on the concentration of I_3 in the bottom of S2.

The only exit for I_3 is the top distillate of column 4 (D4). When this flow rate is decreased to 90% of its nominal value, I_3 will rise and reach a new steady-state value after about 50 h. When D4 is decreased to 70%, I_3 will rise continuously and a new steady state is never reached. The amount of I_3 that is fed to and produced in the plant is higher than the amount that can leave the plant, and therefore I_3 is being built up in the recycles (kind of ''snowball effect"). The limiting value for D4 is about 80% of its nominal value.

An increased DCE flow rate results in a higher production rate of both product and impurities. The impurities will build up in the DCE recycle and go to the top of column S2, from where one part is recycled to R1 (destruction of I_1 and I_2) and another flows to column S4, from where the three impurities can leave the plant.

As shown in Figure 4, the operating window of the distillate flow rate of column S4 has a lower limit of 80% relative to its nominal value. When the flow rate is lower, feed and produced impurity I_3 cannot be purged from the plant anymore; hence, I_3 will build up in the recycles, its concentration finally reaching unacceptably high levels. This is a kind of ''snowball effect'' that occurs to the concentration of impurities rather than to the whole system.

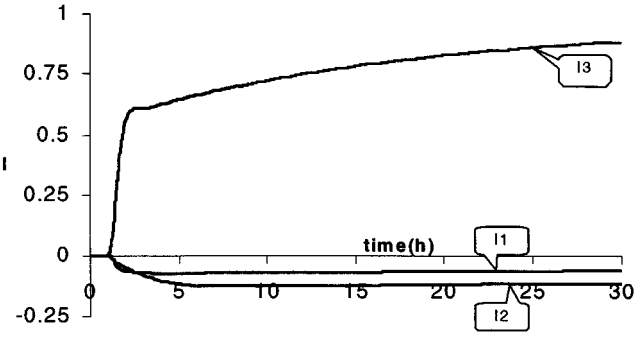

Figure 5. Dynamic response of impurities I_1, I_2, and I_3 (bottom S2) after a scaled step perturbation of 1 on the distillate flow of column S2 in the VCM plant with an extra reactor R4.

The impurities I_1 and I_2 are transformed into heavies in reactor R4, located between column S2 and column S4, so their concentrations will decrease fast when the distillate flow of S2 is increased. In the long term they increase slightly because their lower concentrations lead to less transformation in reactor R1. Impurity I_3 is built up in the recycle and therefore increases.

Flowsheet with Impurity-Destroying Reactor R4. The introduction of reactor R4 has a strong influence on the dynamic behavior of the plant. Because impurities I_1 and I_2 in the top distillate D2 of column S2 are transformed into heavies in R4, increasing flow rate D2 results in a fast drop in I_1 and I_2 in the bottom of S2. At the same time, the feed of column S4 contains less I_1 and I_2, thus allowing more I_3 to leave the plant via the lights directly, compensating for the buildup in the recycle. It will not reach a maximum first (in contrast to the same response in the basic flow sheet, see Figure 2), but goes in a dual fast–slow response to its steady-state value (Figure 5). Now I_1 and I_2 show a minimum, because their transformation into R4 results in lower concentrations and therefore in less transformation into R1, through which the side stream is recycled. The dynamic characteristics of the responses on steps in the other inputs are the same as in the basic flow sheet, but their final values are changed, as can be seen in Table 5.

Dynamic controllability analysis

A scaled linear state space description has been generated using a Taylor series expansion of the differential equations from the dynamic SPEEDUP plant model. This serves as a basis for frequency responses to be calculated in MATLAB.

From Figure 6 it may be seen that the static gains appear to hold well for frequencies up to 0.05 h^{-1}. At frequencies above 10 h^{-1} the system stops responding to disturbances, and feedback control is no longer needed. Besides, the system is not responding anymore to the manipulated variables. For oscillations with a frequency in between, the system responses feature a delay and the magnitudes are lower. This

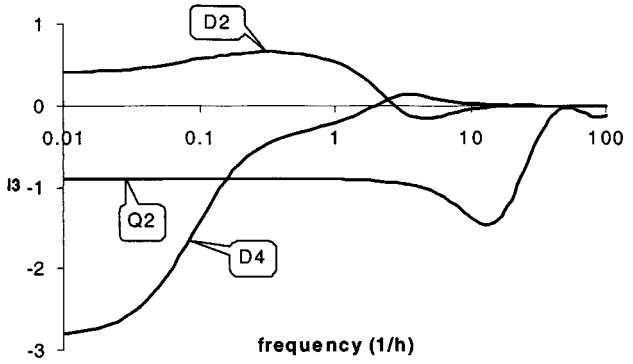

Figure 6. Frequency responses of impurity I_3 to D2, Q2, and D4.

The response of I_3 to an oscillation on D4 already starts to deviate from steady state at a low frequency. Column S4 cannot follow these fluctuations. The response of I_3 to an oscillation on D2 starts to increase at the same frequency. The removal of I_3 by column S4 seems to compensate for the buildup effect of D2 at low frequencies. The response of I_3 to an oscillation on Q2 remains the same for the whole frequency range where feedback control is needed. At frequencies where the system is not responding to D2 and D4 anymore because the recycles cannot follow these fast fluctuations, the effect of Q2 is still equal to that at low frequencies. The magnitude of Q2 on I_3 first increases before also going to zero only at frequencies that correspond to the time constant of the column itself. The effect of Q2 on I_3 is only reduced by the reflux over the top of the column and is hardly affected by recycle interactions.

clearly demonstrates why a steady-state analysis of the plant behavior is inadequate. During plant operation oscillatory disturbances will always occur with frequencies in this range, hence impurity concentrations will always be in a transient.

If we take a closer look at the frequency responses, we can see a clear difference among D2, Q2, and D4. The lights removal by D4 affects the impurity concentrations in the bottom of column S2 through the recycles. At frequencies above 0.05 h^{-1} the large holdups in the main recycle paths damp the effects, and the response of I_3 to D4 starts to deviate from the steady state. This also affects the response of I_3 to D2 (and SS2, not shown). The buildup of I_3 in the short recycle loop through reactor R1 can follow the intermediate frequencies, but the removal of I_3 via D4 does not compensate for this effect any more. This leads to a higher magnitude for the response on D2 (and SS2) between 0.1 and 1 h^{-1}. Its maximum around a frequency of 0.3 h^{-1} corresponds to the maximum in the step response (Figure 2). This recycle also yields a delaying effect, leading to damping of oscillations at frequencies around 2 h^{-1}. There the residence time in reactor R1 corresponds to half a period, and the recycle interactions are such that the responses to D2 (and also D4) are zero. At higher frequencies the direction of these inputs is opposite to steady state, which will complicate feedback control.

The response to the reboiler duty Q2 shows another behavior. It is mainly a result of the interaction between the reboiler and the column S2 itself and is hardly affected by recycle interactions. Therefore the system follows the input changes up to much higher frequencies. At frequencies between 2 and 20 h^{-1}, where the period of the fluctuations is of the same order as the response time of the column, the magnitude of Q2 is increased because the opposite effect of the reflux over the top of the column is damped. The maximum gain around 12 h^{-1} corresponds to the minimum in the step response (6 min; Figure 2). Also, at higher frequencies the reboiler does not affect the impurities anymore.

RGA. In order to analyze the interaction behavior of the system an RGA analysis has been applied. The RGA number, defined as the sum norm (sum of the absolute values of all elements) of the RGA matrix minus the identity matrix, $\|\mathrm{RGA}-\mathrm{I}\|_{\mathrm{sum}}$, is used as indicator. Note that RGA numbers close to zero are preferred over the whole frequency range when diagonal feedback control is concerned, since such values would predict a minimum of interactions. The recycle interactions just indicated have a significant influence on the RGA elements. The direction of responses on inputs D2 and D4 at frequencies between 1 and 10 h^{-1} become opposite to that at steady state (Figure 6). Hence, more interactions between control loops are expected at higher frequencies. This is confirmed by high RGA numbers for the diagonal structures with I_1-Q2, I_2-SS2, I_3-D2, or I_1-Q2, I_2-SS2, I_3-D4 as control loops at these frequencies (Figure 7).

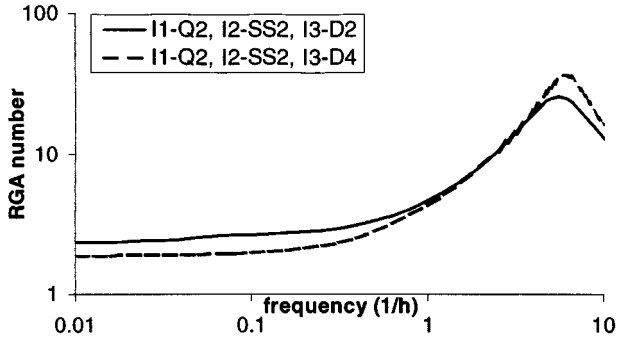

Figure 7. RGA number of two alternative control structures of the VCM plant.

This figure shows that at low frequencies the control structure with D4 has fewer interactions than the one with D2. At higher frequencies, interaction between the different control loops increase rapidly for both structures.

Diagonal controller performance

Steady-state and dynamic RGA analyses have been used to study the interactions between control loops and to select the preferred input–output pairings. In this way two different control structures have been selected for the VCM plant. Now the performance of these structures will be studied in terms of the controller errors. These should be kept between the scaled bounds $[-1, 1]$ under disturbances and reference changes.

An approximation of the controller errors e in terms of the disturbances d and the reference values r is given by

$$e = SG_d d - Sr \approx \tilde{S}\tilde{G}_d d - \tilde{S}\Gamma r, \qquad (1)$$

where the sensitivity matrix S is decoupled and approximated by a product of two terms, $S \approx \tilde{S}\Gamma$. The diagonal sensitivity matrix $\tilde{S} = \mathrm{diag}\{1/(1 + k_i g_{ii})\}$, g_{ij} being the open-loop gain and k_i the controller gain, has only diagonal elements. This allows evaluation of the *individual* controllers independent from each other, which is convenient for tuning. The PRGA ($\Gamma = \tilde{G}G^{-1}$, where $\tilde{G}$ contains only the main diagonal of G) and CLDG ($\tilde{G}_d = \Gamma G_d$) are counting for the interactions between the control loops, without actually closing them. Notice that when all PRGA and CLDG elements for a certain control loop are below 1, no control is actually needed since then the error will never exceed its bounds.

When the PRGA and CLDG elements exceed 1, the controller gain k_i can be selected such that the largest element of the products $\tilde{S}\tilde{G}_d$ and $\tilde{S}\Gamma$ for the specific loop becomes equal to 1. This is the minimum controller gain that will keep the error between its bounds under all disturbances and reference changes.

These tools have been applied to the selected control structures for the VCM plant.

Performance Relative Gain Array. Figure 8 shows the effect of a setpoint change of impurity I_3 between the bounds $[-1, 1]$ as a function of frequency. When the diagonal control structure I_1-Q2, I_2-SS2, I_3-D2 is implemented in the base-case flow sheet (Figure 8a), the setpoint tracking of I_3 in itself is effective at low frequencies; while the unwanted impact on I_1 and I_2 is acceptable, that on I_2 is somewhat higher. At higher frequencies, where the interactions between the control loops become significant, all impurities will exceed their bounds, so feedback control is no longer effective. When the alternative diagonal structure I_1-Q2, I_2-SS2, I_3-D4 is used (Figure 8b), again I_3 is controlled effectively at low frequencies, while im-

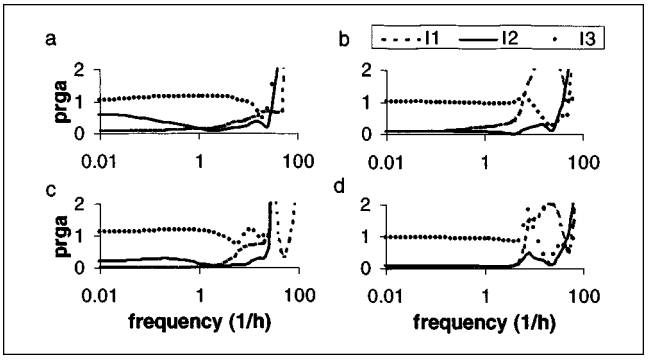

Figure 8. Performance relative gain array elements for the effect of a reference change of I_3 on the outputs.

(a) Base case with diagonal control structure I_1-Q2, I_2-SS2, I_3-D2; (b) base case with diagonal control structure I_1-Q2, I_2-SS2, I_3-D4; (c) alternative with reactor R4 and diagonal control structure I_1-Q2, I_2-SS2, I_3-D2; (d) alternative with reactor R4 and diagonal control structure I_1-Q2, I_2-SS2, I_3-D4. Part (a) shows that the reference change of I_3 affects the impurities I_1 and I_2 only slightly. This influence is even less when another control structure (part b) or another flow-sheet structure (parts c and d) is used, although this is not really needed. In all cases, control of I_1 and I_2 is not needed when the reference value of I_3 is changed.

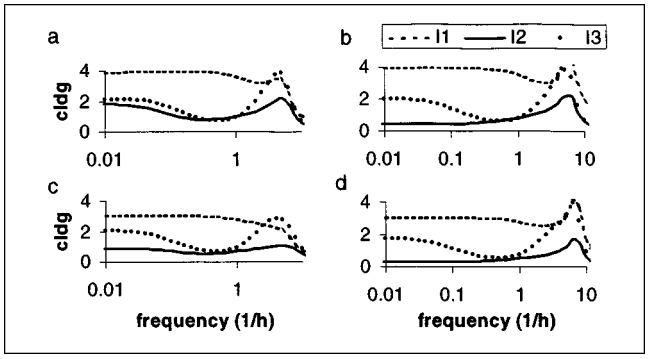

Figure 9. Closed-loop disturbance gains for the feed disturbance F_{DCE} on the outputs.

(a) Base case with diagonal control structure I_1-Q2, I_2-SS2, I_3-D2; (b) base case with diagonal control structure I_1-Q2, I_2-SS2, I_3-D4; (c) alternative with reactor R4 and diagonal control structure I_1-Q2, I_2-SS2, I_3-D2; (d) alternative with reactor R4 and diagonal control structure I_1-Q2, I_2-SS2, I_3-D4. Part (a) shows that all three impurities are affected by the feed disturbance and need to be controlled. This is in contrast with part (b), showing that I_2 is hardly affected by the feed disturbance when I_3 is controlled by D4 instead of D2. As a result of the controller interactions, I_2 will be kept within its bounds, and it does not need to be controlled for this disturbance. The introduction of reactor R4 (parts c, d) suppresses the closed-loop disturbance gains of all three impurities. Again, I_2 does not need to be controlled, this time for both control structures.

purities I_1 and I_2 are only slightly affected. However, I_1 will exceed bounds at a somewhat lower frequency than before. Note that although both structures show violations at high frequencies, this is not expected to be a problem during operation, since the setpoint of the initiator for the cracking process is not normally changed at such high frequencies. In conclusion, the PRGA analysis shows both diagonal structures to be nearly equivalent: if only I_3 is controlled on setpoint, the other impurities are automatically kept within their bounds, so no additional control action is required.

Now, it is interesting to see the impact of a flow-sheet change—the addition of an extra impurity-destroying reactor R4—on the setpoint tracking performance, when the *same* two control structures are implemented. The performance of I_1-Q2, I_2-SS2, I_3-D2 (Figure 8c) is similar to that of the same structure in the base-case flow sheet (Figure 8a), although the unwanted impact on I_1 and I_2 is somewhat smaller. The same holds for the second diagonal control structure, I_1-Q2, I_2-SS2, I_3-D4 (Figure 8d), which shows a similar performance as that structure in the base case (Figure 8b). In conclusion, the introduction of the extra reactor R4 in the alternative flow sheet has only a minor improving effect on the performance of the diagonal controller when setpoint tracking is concerned.

Closed-Loop Disturbance Gain. The CLDG analysis has been applied in the VCM example for two disturbances: the feed stream F_{DCE} and the concentration on impurity I_3 in this feed stream, X_{I_3}, under the two diagonal control structures mentioned earlier, for both flow-sheet alternatives; the results are shown in Figures 9 and 10. Figure 9a, which shows all CLDG elements to be above one, indicates that extra control action is necessary to reject disturbances of the feed flow F_{DCE} on any of the impurity levels for the structure I_1-Q2, I_2-SS2, I_3-D2 in the base case. For the other disturbance (X_{I_3}), Figure 10a indicates that impurity I_1 in this case automatically stays within acceptable bounds when only I_2 and I_3 are controlled; hence the system is almost indifferent to the presence or absence of the controller I_1-Q2. Figure 9b shows that the behavior of the alternative control structure I_1-Q2, I_2-SS2, I_3-D4 is improved with respect to disturbance F_{DCE}, since here impurity I_2 does not require control, while I_1 and

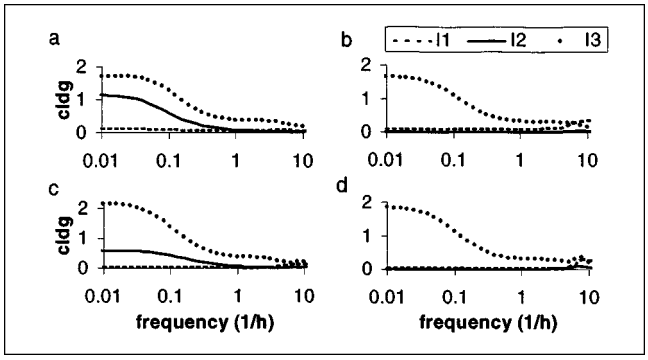

Figure 10. Closed-loop disturbance gains for the impurity disturbance X_{I_3} on the outputs.

(a) Base case with diagonal control structure I_1-Q2, I_2-SS2, I_3-D2; (b) base case with diagonal control structure I_1-Q2, I_2-SS2, I_3-D4; (c) alternative with reactor R4 and diagonal control structure I_1-Q2, I_2-SS2, I_3-D2; (d) alternative with reactor R4 and diagonal control structure I_1-Q2, I_2-SS2, I_3-D4. According to part (a), both I_2 and I_3 need to be controlled at low frequencies when D2 is used to control I_3. This is in contrast with part (b), which shows that I_2 does not need controlling when D4 is used to control I_3. Part (c) shows that introduction of reactor R4 makes the closed-loop disturbance gain of I_3 larger, but that of I_2 is lower. Part (d) shows that in combination with the alternative control structure, both I_1 and I_2 are not affected by the impurity disturbance.

I_3 still do. Figure 10b also shows improvement in the other disturbance, since under the alternative structure only I_3 needs control, while I_2 and I_1 do not. Hence, in the base-case flowsheet the structure I_1-Q2, I_2-SS2, I_3-D4 performs best, since impurity I_2 never requires control. Figure 9c shows the result for the alternative flowsheet containing reactor R4. Disturbance F_{DCE} with structure I_1-Q2, I_2-SS2, I_3-D2 requires only impurities I_1 and I_3 to be controlled, so the controllability of this flowsheet is slightly better than that of the base case. Figure 10c shows this situation to be improved for the disturbance X_{I_3}, only requiring control for I_3. Figure 9d and Figure 10d indicate that the alternative control structure I_1-Q2, I_2-SS2, I_3-D4 does not lead to further improvement in this flowsheet, as it did in the base case. For disturbance F_{DCE}, I_1 and I_3, and again for X_{I_3}, only I_3 has to be controlled. In conclusion, both the alternative control structure and the alternative flowsheet structure perform better than the base case. Choosing the best alternative, I_3 always has to be controlled with D4, while for disturbance F_{DCE}, I_1 also has to be controlled with Q2.

Relative Disturbance Gain. The ratio between the closed-loop disturbance gain and the open-loop disturbance gain, given the change in input–output behavior due to diagonal feedback control, is called the *relative disturbance gain* (RDG). The elements of this matrix are preferably smaller than one, which would mean that the interactions between the controllers are such that they reduce the apparent effect of the disturbance. In such cases relatively small gains are sufficient for the individual loops. They may also be larger than 1, however, indicating that the apparent effect is enhanced instead, implying high gains for the loops concerned. Assuming the structure I_1-Q2, I_2-SS2, I_3-D4 in the base-case flowsheet, RDG values have been plotted in Figure 11 for all three impurities. For the concentration of impurity I_3 in the DCE feed (X_{I_3}) as the disturbance, at low frequencies the RDG values are below one, so the system can be controlled with small controller gains. At frequencies between 1 and 10 h^{-1} the RDG elements rise to high values, indicating that the direction of the controller interactions is opposite, which complicates control of the impurities. At these frequencies control would not even be possible, but this is not a problem since according the CLDG elements, the impurities are automatically kept within their bounds, so control is also not required. The other disturbance, the step on the DCE feed (F_{DCE}), also gives rise to RDG elements less than one at low frequencies, but they are not so high at intermediate frequencies. So, for this disturbance the apparent effect of the controller interactions is such that the open-loop behavior is less affected.

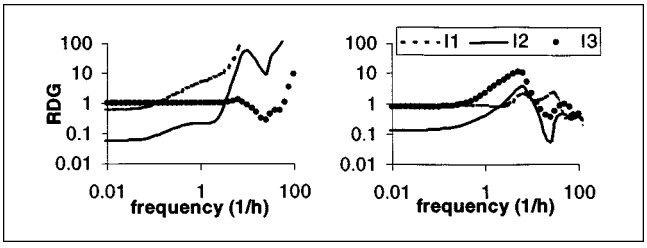

Figure 11. Relative disturbance gains for the basic flowsheet with diagonal control structure I_1-Q2, I_2-SS2, I_3-D4, left for X_{I_3}, right for F_{DCE}.

The left panel shows that the apparent effect of the disturbance X_{I_3} on I_2 with this control structure implemented is reduced considerably at low frequencies, so a low controller gain would be sufficient. At higher frequencies, the closed-loop disturbance gains are higher than the open-loop disturbance gains, due to negative controller interactions. It should be realized that the absolute values are lower in this frequency range and therefore no control was needed here. The right panel shows that the apparent effect of the flow disturbance on I_2 with this control structure implemented is also reduced markedly at low frequencies, so a low controller gain would be sufficient. At higher frequencies, the closed-loop disturbance gains are again higher than the open-loop disturbance gains, due to negative controller interactions, but this effect is weaker than it is for X_{I_3}.

Especially the RDG values of I_2 are very small for both disturbances at low frequencies. The controller interactions are such that the apparent effect of the disturbances on I_2 is reduced enormously and only small controller gains are needed. This is in agreement with the conclusion from the CLDG analysis that I_2 does not need to be controlled because it is automatically kept within its bounds by the controller interactions.

Tuning the diagonal controller

Since the PRGA elements of the only relevant reference change, that of I_3, were below 1, the tuning will be based on the CLDG only. In order to keep the error within its bounds, k_i has to be selected such that $(1 + k_i g_{ii})$ is equal to or larger than $\tilde{g}_{di}$ for all disturbances in the frequency domain of interest.

This has been carried out for the VCM case. From the previous section it was concluded that for the base-case flowsheet and control structure I_1-Q2, I_2-SS2, I_3-D2 impurities I_2 and I_3 always would have to be controlled. Now, we investigate whether this is indeed possible, first for I_2 then for I_3. Figure 12 shows the impact on impurities I_2 and I_3 for changes in the two disturbances analyzed before: F_{DCE} and X_{I_3}, the former having a more serious impact. Figure 12a shows the open-loop gain of the manipulated variable to control I_2, in this structure $g_{22} = \text{SS2}$. Since this gain is lower

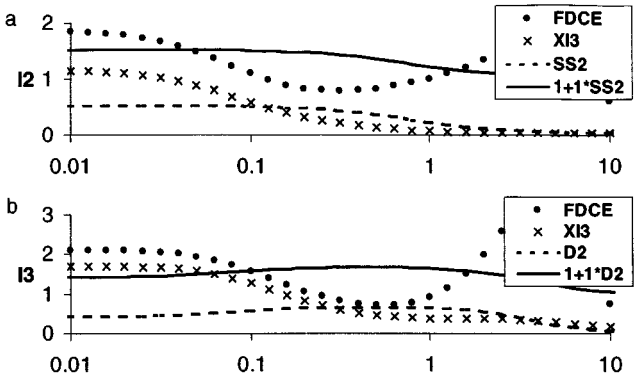

Figure 12. Tuning of diagonal control structure I_1-Q2, I_2-SS2, I_3-D2 with CLDG.

When D2 is used to control I_3, SS2 and D2 do not have enough magnitude to keep I_2 and I_3 within their bounds with the maximum controller gain of 1.

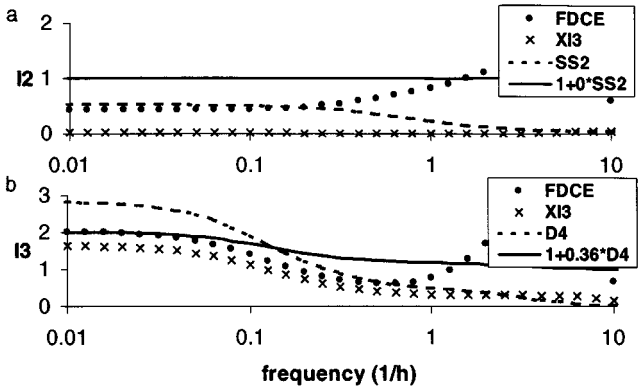

Figure 13. Tuning of diagonal control structure I_1-Q2, I_2-SS2, I_3-D4 with CLDG.

When D4 is used instead of D2, I_2 does not need control (gain zero) and I_3 can be controlled within its bound with a scaled controller gain of 0.36.

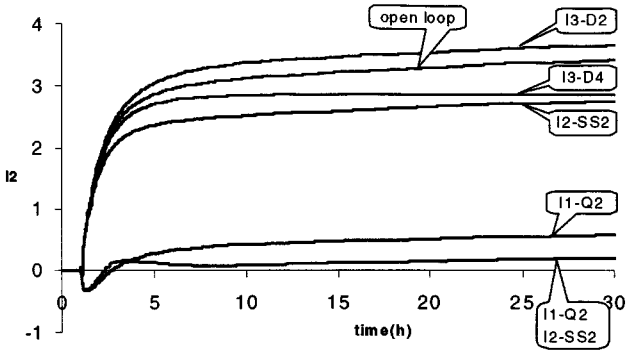

Figure 14. Closed-loop dynamic responses of I_2 to a step disturbance on the DCE feed.

Implementing only controller I_1-Q2 keeps I_2 within its bounds, while implementing only controller I_2-SS2 does not, and SS2 will reach its bound. When both controllers are combined (I_1-Q2 and I_2-SS2), I_2 is kept within its bounds. When the controller I_3-D2 is the only active one, I_2 is increased relative to the open-loop response, while controller I_3-D4 has a reducing effect on I_2.

than the CLDG curves, insufficient input magnitude is available to control I_2 on setpoint. On the other hand, the curve of $(1 + k_2 g_{22})$ for a maximum (scaled) controller gain of 1 lies entirely above the CLDG of the impurity disturbance of the DCE feed $\tilde{g}_{d2}$ $(d = X_{I_3})$, so this disturbance can be rejected and control of I_2 within bounds is possible for this disturbance. However, at low frequencies $(1 + k_2 g_{22})$ is smaller than $\tilde{g}_{d2}$ $(d = F_{DCE})$, so there is lack of control power for the feed disturbance and I_2 will move outside its bounds. Figure 12b shows a similar plot for impurity I_3, which in this control structure is to be controlled with D2. It shows that D2 lacks control power to control either of the two disturbances on setpoint or within bounds. In conclusion, where the previous analysis indicated the necessity of controlling I_2 and I_3, it finally turns out from the tuning procedure that control within bounds is not possible in this case.

Regarding the alternative control structure I_1-Q2, I_2-SS2, I_3-D4, it was concluded in the previous section that control was never required for I_2, while control is always needed for I_3 and sometimes for I_1. Figure 13 confirms this conclusion for I_2, showing $(1 + k_2 g_{22})$ to always be larger than $\tilde{g}_{d2}$, even with zero gain. In contrast, impurity I_3 needs control, and it indeed appears to be possible for a controller gain even below the maximum: $k_3 = 0.36$.

In conclusion, the closed-loop controllability tools are indeed able to discriminate between various control and flowsheet alternatives, proving that the two flowsheets are controllable with the alternative control structure, while they are not with the base-case structure. The closed-loop tuning technique proved to confirm this conclusion and was successfully used to tune the alternative controller with respect to the control of I_3 with D4.

Closed-loop simulations

Closed-loop simulations with the nonlinear dynamic model were carried out so they could be compared with the results of the controllability analysis. Figures 14 and 15 show the response of impurities I_2 and I_3, respectively, on a feed disturbance F_{DCE} for the base-case flowsheet and several control structures. Implementing only one controller, I_1 with Q2, automatically yields effective control of I_2, but this is not so for I_3, although the response is suppressed to some extent. Again assuming a 1-controller system, but this time controlling I_2 with SS2, gives surprisingly bad results for I_2 itself, and the result for I_3 is even worse. Another 1-controller system that is evaluated, I_3 with D2, produces a bad performance for both impurities. However, controlling I_3 with D4 works out very well for I_3, but only poorly for I_2. Hence, none of the 1-controller systems works satisfactorily for both impurities, which is in agreement with the controllability analysis. Two 2-controller systems have been implemented. The I_1-Q2, I_2-SS2 system performs very well for I_2 but does not keep I_3 within bounds, even when a third controller, I_3-

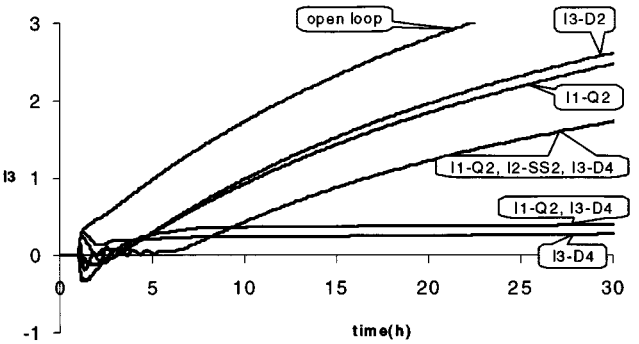

Figure 15. Closed-loop dynamic responses of I_3 to a step disturbance on the DCE feed.

Control of I_1 with Q2 reduces the effect of the disturbance on I_3 more than when I_3 itself is controlled with D2. In this case, D2 reaches its bound and I_3 cannot be controlled further. This is still the case when all three controllers I_1-Q2, I_2-S2, and I_3-D2 are implemented. However, I_3 can be controlled with D4. Because this also reduced the disturbance effect on impurity I_1, the closed-loop response of I_3 with both controllers I_1-Q2 and I_3-D4 is slightly higher, but the impurity is kept within its bounds $[-1, 1]$.

D2, is added, which is in agreement with the controllability results, which predict bad performance for all impurities in the case of control structure I_1-Q2, I_2-SS2, I_3-D2. The 2-controller system I_1-Q2, I_3-D4 works well for all impurities, which also fits with the controllability analysis, which indicates a better performance for the alternative control structure I_1-Q2, I_2-SS2, I_3-D4. Hence, it is also confirmed that a third controller, to control I_2, is not necessary.

Closed-loop simulations with the controller structure I_1-Q2 and I_3-D4 implemented in the flow sheet with reactor R4 showed that the disturbances are reduced by about the same amount. The dynamic profiles are comparable with the base case. However, since the nominal values of impurities I_1 and I_2 are lower in this flowsheet structure, their values stay lower in the closed-loop simulations with disturbances. Therefore, this alternative flowsheet is preferable above the base case, which again confirms the controllability conclusions.

Conclusions

In this article we have presented a simulation-based methodology for evaluating flowsheet design and control alternatives with regard to their controllability and closed-loop behavior. The systems approach is illustrated with an industrial case study on the removal of impurities in a balanced VCM process. It is shown that the combination of steady-state and dynamic simulations, together with a linear controllability analysis in the frequency domain, improves our understanding of the behavior of a large plant with a complex recycle structure to a greater extent than extensive steady-state simulations only.

Furthermore, it is shown that the material balance of impurities in the VCM plant is a plantwide problem. It is demonstrated how the interaction between recycles can be exploited to create flowsheet and control alternatives with feasible plantwide control properties. Using the positive-feedback effects of the recycle streams and the negative feedback effects of chemical reactors and exit streams leads to an alternative flowsheet design and control structure with acceptable control properties. In this structure the manipulated variables belong to different units, as could be expected from the steady-state analysis. The interaction between the controllers is such that all three impurities can be kept within their bounds with only two controllers implemented. This was predicted by the controllability analysis and confirmed by the closed-loop simulations, but doing a steady-state analysis alone turned out to be insufficient to obtain this result. This proves that a linear controllability analysis in the frequency domain with tools like PRGA and CLDG is useful and is capable of discriminating between flowsheet and control alternatives in an effective way. In particular, using the controllability analysis it appeared that the problems mainly come from the interaction between the different units in the flowsheet. This also illustrates the difference in nature between the controllability characteristics of a plant as compared to those of a single column. Column dynamics may be complex as well, but they do not offer such a wide variety of problem causes distributed in unknown ways over the system, and consequently they do not possess so many unexpected ways of solving those problems. These solutions also are not as easily detected by intuitive means, and stress the importance of controllability tools even more.

The case study focused on a large complex plant, the Vinyl Chloride Monomer plant. It showed that the material balance of impurities is always in a transient state, with time constants on the order of days, making a dynamic analysis unavoidable. The steady-state analysis suggested using the side stream SS2 as a manipulated variable to control one of the impurities (I_2). However, dynamic simulations showed that this gives a serious inverse response. Controllability analysis showed the shortcomings of input magnitude, and closed-loop simulations showed that a new steady state could not even be achieved. Changing the control loop for another impurity, using D4 instead of D2 to control I_3, reduces the apparent effect of the disturbance such that control of I_2 is no longer needed. The improved performance of this alternative could never have been predicted by intuition.

Literature Cited

Barton, G. W., W. K. Chan, and J. D. Perkins, ''Interaction Between Process Design and Process Control: The Role of Open-Loop Indicators,'' *J. Process Control*, **1**, 161 (1991).

Buckley, P. S., ''Material Balance Control in Recycle Systems,'' *Instrum. Technol.*, **5**, 29 (1974).

Denn, M. M., and R. Lavie, ''Dynamics of Plants with Recycle,'' *Chem. Eng. J.*, **24**, 55 (1982).

Dimian, A., ''Use Process Simulation to Improve Plant Operations,'' *Chem. Eng. Prog.*, **90**(9), 58 (1994).

Dimian, A., A. J. Groenendijk, and P. Iedema, ''System Analysis in Handling Impurities in Complex Plants,'' *Comput. Chem. Eng.*, **20**, S805 (1996).

Downs, J. J., ''Distillation Control in a Plantwide Environment,'' *Practical Distillation Control*, W. L. Luyben, ed., Van Nostrand Reinhold, New York, p. 413 (1992).

Gilliland, E. R., L. A. Gould, and T. J. Boyle, ''Dynamic Effects of Material Recycle,'' *Preprints JAC*, Joint Automatic Control Conference, Stanford, CA, p. 140 (1964).

Joshi, S. K., and J. M. Douglas, ''Avoiding Accumulation of Trace Components,'' *Ind. Eng. Chem. Res.*, **31**, 1502 (1992).

Luyben, M. L., and W. L. Luyben, ''Design and Control of Complex Process Involving Two Reaction Steps, Three Distillation Columns, and Two Recycle Streams,'' *Ind. Eng. Chem. Res.*, **34**, 3885 (1995).

Luyben, W. L., ''Dynamics and Control of Recycle Systems: 1. Simple Open-Loop and Closed-Loop Systems,'' *Ind. Eng. Chem. Res.*, **32**, 466 (1993a).

Luyben, W. L., ''Dynamics and Control of Recycle Systems: 2. Comparison of Alternative Process Design,'' *Ind. Eng. Chem. Res.*, **32**, 476 (1993b).

Luyben, W. L., ''Dynamics and Control of Recycle Systems: 3. Alternative Process Designs Including Ternary Systems,'' *Ind. Eng. Chem. Res.*, **32**, 1142 (1993c).

Luyben, W. L., and B. D. Tyreus, ''Dynamics and Control of Recycle Systems: 4. Ternary Systems with One or Two Recycle Streams,'' *Ind. Eng. Chem. Res.*, **32**, 1154 (1993).

Lyman, P. R., and C. Georgakis, ''Plantwide Control of the Tennessee Eastman Problem,'' *Comput. Chem. Eng.*, **19**, 321 (1995).

Mizsey, P., and Z. Fonyo, ''Assessing Plant Operability During Process Design,'' *Computer-Oriented Process Engineering*, Elsevier, Amsterdam, p. 411 (1991).

Mohideen, M. J., J. D. Perkins, and E. N. Pistikopoulos, ''Optimal Design of Dynamic Systems Under Uncertainty,'' *AIChE J.*, **42**(8), 2251 (1996).

Morud, J., and S. Skogestad, ''The Dynamic Behavior of Processing Units,'' *Comput. Chem. Eng.*, **17**, S529 (1993).

Morud, J., ''Studies on the Dynamics of Integrated Plants,'' PhD Thesis, Univ. of Trondheim, Trondheim, Norway (1995).

Papadurakis, A., M. F. Doherty, and J. M. Douglas, ''Relative Gain

Array for Units in Plants with Recycle,'' *Ind. Eng. Chem. Res.*, **26**, 1259 (1987).
Price, R. M., P. R. Lyman, and C. Georgakis, ''Throughput Manipulation in Plantwide Control Structures,'' *Ind. Eng. Chem. Res.*, **33**, 1197 (1994).
Skogestad, S., and I. Postlethwaite, *Multivariable Feedback Control*, Wiley, New York (1996).
Verykios, X., and W. L. Luyben, ''Steady-State Sensitivity and Dynamics of a Reactor/Distillation Column System with Recycle,'' *ISA Trans.*, 31 (1978).
Wolff, E., and S. Skogestad, ''Controllability of Integrated Plants Applied to Recycle Systems,'' AIChE Meeting, New Orleans, LA (1992).
Wolff, E., ''Studies on Control of Integrated Plants,'' PhD Thesis, Univ. of Trondheim, Trondheim, Norway (1994).
Yi, C. K., and W. L. Luyben, ''Evaluation of Plant-Wide Control Structures by Steady State Disturbances Sensitivity Analysis,'' *Ind. Eng. Chem. Res.*, **34**, 2393 (1995).

Manuscript received Mar. 15, 1999, and revision received Sept. 13, 1999.